

Rupture Process of the 2011 Mw9.0 Tohoku Earthquake And Strong Motion Simulation from the Viewpoint of NPP Seismic Design



Changjiang Wu, Hideaki Tsutsumi

Japan Nuclear Energy Safety Organization (JNES), Japan

Hongjun Si, Yusuke Saijo

Kozo Keikaku Engineering Inc., Japan

SUMMARY:

Rupture process of the 2011 Mw9.0 Tohoku earthquake is estimated by using long-period waveform inversion. Our results show that the earthquake produced large dislocations of nearly 70m in the up-dip region, a relatively shallow area along the Japan trench, consistent with the source models inferred from tsunami observation. On the other hand, a source model constructed by strong motion simulation is composed of five asperities (or strong motion generation areas, SMGA) in the down-dip region. In contrast to the moment magnitude of 9.0 estimated from the long-period waveform inversion, each SMGA is of moment magnitude not larger than 8.0. It suggests a frequency-dependent rupture pattern featured with short-period wave radiation concentrated in the down-dip region and long-period wave radiation in the up-dip region. This finding is of great importance for NPP seismic design since asperities in the previous source models for seismic design are mainly in the down-dip region.

Keywords: The 2011 Tohoku earthquake, rupture process, strong motion, design basis ground motion

1. INTRODUCTION

Nuclear energy is a main source of electricity in Japan. The nuclear power plants (NPP) had been providing some 30% of the country's electricity before 2011. Because of high seismicity in Japan, great attention has been paid to NPP seismic design. In 1978, the Atomic Energy Commission (AEC) issued a seismic design regulatory guide and required to formulate design basis ground motions (DBGM) of two levels, i.e., S1 for the maximum earthquake and S2 for the extreme case, of which the latter had been used for seismic design of safety related high-class (important) structures, systems, and components (SSC). Regulation revision for appropriate reflection of the most up-to-date knowledge is expressly stipulated in this guide. In light of the 1995 Kobe earthquake as well as a decade accumulation of high-quality strong motion observation, the Nuclear Safety Commission (NSC) revised the guide in 2006, extending the geological age required for active fault evaluation, integrating the two level DBGMs (S1 and S2) into the DBGM Ss with inclusion of the source rupture modelling method (Irikura, 1994; Irikura and Miyake, 2001), and expanding the contents of the high-class SSCs.

In 2007, the year following the revision, the Kashiwazaki-Kariwa NPP, the biggest NPP site in the world, withstood the Niigata-ken Chuetsu-oki earthquake, which generated a strong seismic shaking significantly exceeding the DBGM as indicated by the response spectra comparison at the level of the foundation base mat in all units. Investigation reports of the International Atomic Energy Agency (IAEA, 2008) concurred that the integrity of SSCs important to safety was confirmed for the earthquake in spite of the strong seismic motions and that areas of significant margin were identified through expert judgement and detailed physical inspections. As one of lessons learned from this earthquake, the agency's reports also pointed out that the estimation of ground motions from near-site faults requires the incorporation of source characteristics including fault mechanism, directivity effects, and three-dimensional rupture characteristics. Since the 2006 guide adopts the source rupture modelling method which is advantageous in this kind of problems, earthquake engineers are confident in appropriate evaluation of DBGM in line with the 2006 guide.

The 2011 off the Pacific coast of Tohoku earthquake, however, greatly affected the public confidence

in NPP safety because the strong shaking and the sequent huge tsunami directly resulted in a Station Blackout accident at the Fukushima Daiichi NPP. According to the Japan Meteorological Agency (JMA), the earthquake occurred at 14:46 on March 11, 2011 with a depth of 23.7km in the sea area off Miyagi Prefecture. Though the so-called Miyagi-oki earthquake had long been warned by the Headquarters for Earthquake Research Promotion (HERP), the size of the Tohoku megathrust earthquake was totally beyond seismologists' expectation. As Fig.1 showed, wide-range areas experienced strong shakings of seismic intensity larger than 5 (in JMA scale). Including the abovementioned Fukushima Daiichi NPP, all reactors under operation at the Onagawa, Fukushima Daini NPP, and Tokai Daini NPPs were automatically shutdown during the earthquake.

As a study on the 2011 Tohoku earthquake, we first focus on the source model on the basis of long-period waveform inversion since an appropriate source model is of great importance for the source rupture modelling method. On the other hand, understanding of the characteristics of short-period seismic waves is important for NPP seismic safety. For this purpose, we also construct a strong motion generating source model by simulation of short-period ground motions. Then we discuss the applicability of the rupture modelling method for DBGGM formulation as well as issues to be solved in future from the viewpoint of NPP seismic design.

2. THE RUPTURE PROCESS ESTIMATED FROM LONG-PERIOD WAVES

2.1 Tectonic Setting

The Tohoku earthquake occurred on the plate boundary along the Japan trench (See Fig.1, right), where the Pacific plate subducts beneath the Okhotsk plate at a rate of 8cm/yr (Apel et al., 2006). Recent studies on historical earthquakes in this area (e.g., Yamanaka and Kikuchi, 2004; Wu et al., 2008) suggested that the strain energy associated with the plate movement has been released by repeated ruptures of the asperities concentrated deeper than 30km. Strong coupling of the deep region of the plate boundary is also supported by the studies on plate movements using the Global Positioning System observation data (e.g., Nishimura et al, 2004). Meanwhile, relatively frequent occurrence of large earthquakes in the deep region and less frequent occurrence of tsunami earthquakes which slowly rupture the shallow section led to the wrong belief that the shallow region of the plate boundary is weakly coupled and a Tohohoku type mega earthquake was not considered to occur in this area.

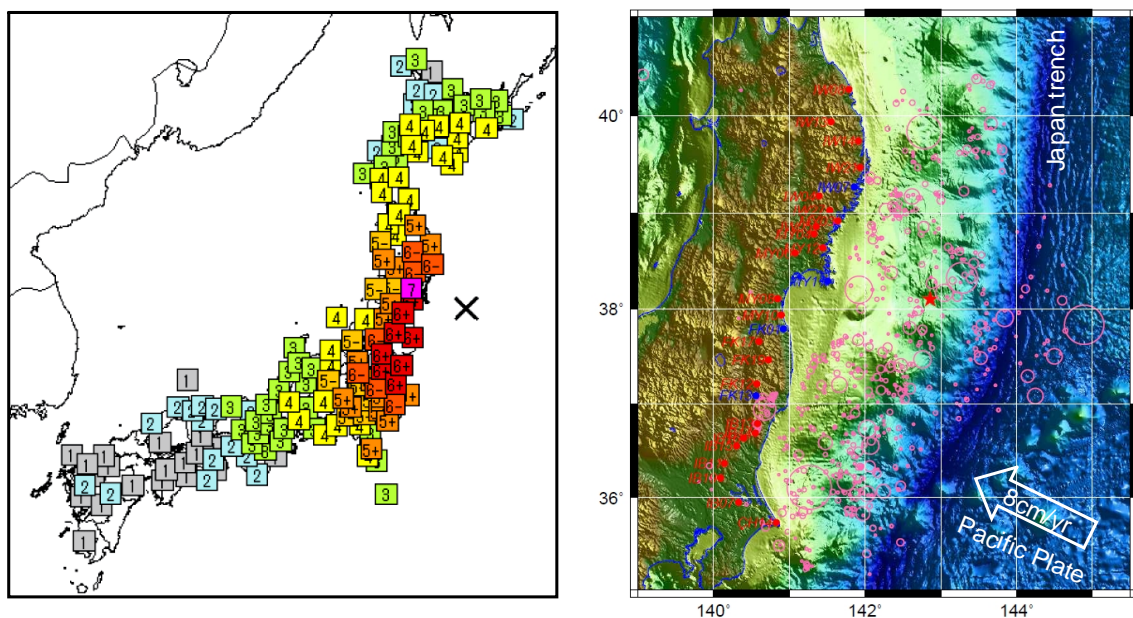


Figure 1. Seismic observation of the Tohoku earthquake. Left: Distribution of seismic intensities (in JMA scale) ; Right: Distribution of aftershock epicentres (up to May 31, 2011 with magnitude above 5.0).

2.2 Strong Motion Data

A large number of strong motion data were recorded during the Tohoku earthquake by the K-NET (Kinoshita, 1998) and KiK-net (Aoi et al., 2000) seismograph networks in Japan Islands, which are operated by the National Research Institute for Earth Science and Disaster Prevention (NIED). It was the first Mw9-class earthquake observed by such densely-spaced seismic networks. In this study, we use the strong motion data recorded at 4 K-NET stations and by 23 KiK-net underground seismographs. The accelerograms with duration of 300 seconds are bandpass filtered (0.008Hz ~ 0.1Hz) and integrated into velocity waveforms.

2.3 Source Model and Inversion Results

2.3.1 Underground ground structure model and Green's functions

In order to take account of the heterogeneity of the Conrad and Moho discontinuity distribution beneath the Japan Islands, station-specific velocity structure models are constructed based on previous studies (Abdelwahed and Zhao, 2007) as well as the KiK-net borehole log data of P and S-wave velocities. The Green's function are calculated using the station-specific horizontally layered model and the reflection/transmission matrix method (Kennett and Kerry, 1979).

2.3.2 Geometric characteristics of the plate boundary and the fault model

We use a bending fault model with a size of 450km length and 240km width on the basis of aftershock distribution (Fig.1). The bending geometry along the strike is directly inferred from the strike of the Japan trench, whereas the depth-dependent dip angles (i.e., 11° for depth <25 km and 22° else) are inferred from previous studies on the geometry of the plate boundary interface using ocean bottom seismometer data (e.g., Shinohara et al., 2005).

2.3.3 Inversion method and results

The fault plane is divided into 30km square subfaults. Source time function on each subfault is expressed by 16 half-overlapped 8-second-width isosceles triangles. The starting time of the first time window is fixed by assuming the maximum average rupture velocity of 2.5km/s. A nonnegative linear inversion method is used with smoothing constraints on the final slip values. Refer to Wu et al., 2004 for detailed inversion procedure.

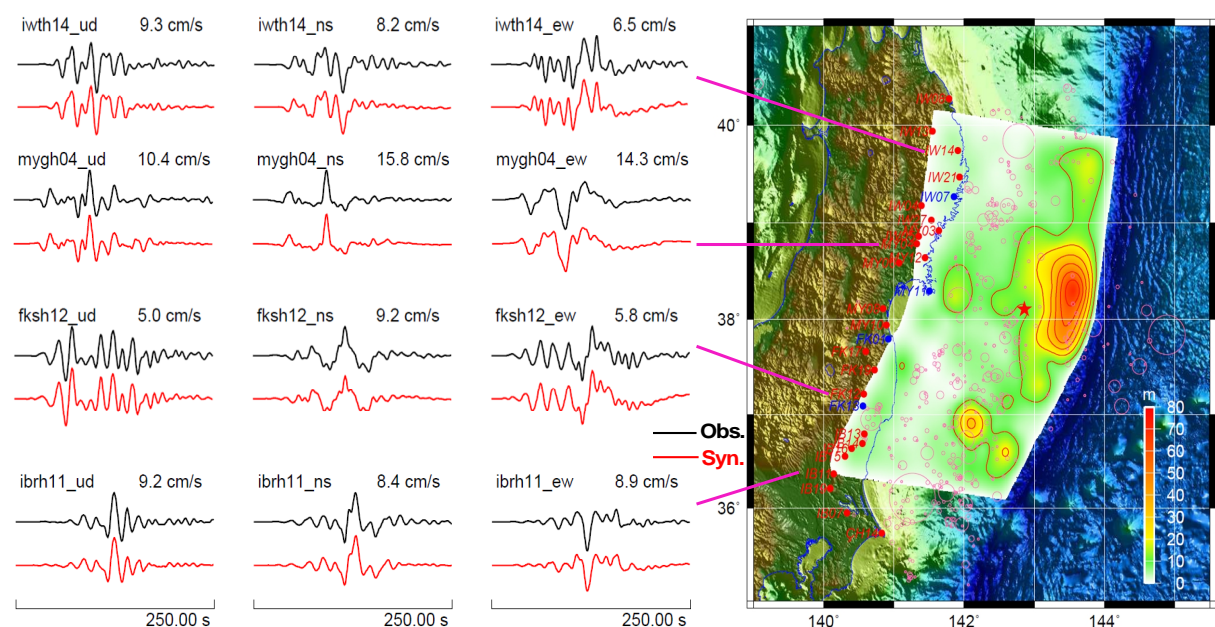


Figure 2. Waveform comparison and slip distribution map. Left: Comparison of synthetic waveforms (red) with the observation data (black); Right: Slip distribution inferred from the long-period seismic waves (<0.1 Hz).

Fig.2 shows the projection of slip distribution to the surface. Our results indicate that the rupture was mainly confined in the downdip region west to the hypocenter (the red solid star in Fig.2) in the first 50 seconds, then propagated to the shallow region and produced very large slip (the maximum value of more than 60m). The large slip was concentrated in the shallow region along the Japan trench, on the east of the hypocenter. For the sake of comparison, we denote the above source model as the slip model (For comparison with the tsunami source model, refer to Sugino, et al., 2012). As can be seen from the examples of waveform comparison showed in the left side of Fig.2, the synthetic waveforms fit well the observation data.

3. SOURCE MODEL FROM STRONG MOTION SIMULATION

Note that the above analysis focuses on the strong motions with periods larger than 10 seconds. On the other hand, the dominant frequency of seismic ground motions important to NPP seismic safety ranges from 2~10Hz, a frequency band unable to deal with by the analytical method due to uncertainties in the underground structure model and the source characterization. To construct a source model for short-period ground motions, the empirical Green's function (EGF) method based on the scaling laws of source parameters (Yokoi and Irikura, 1991) is applied in this study. As indicated from the analyses of arrival times of the observed multiple pulse waves (e.g., Kurahashi and Irikura, 2011; Kawabe et al., 2011), at least five source areas could be identified as the strong motion generation areas (SMGA). Fig. 3 shows the distribution of SMGAs assumed in this study. Consequently, five moderate earthquakes (see Table 2) occurring in the vicinity of the five SMGAs are selected as the EGF earthquakes to better represent the source effects of each SMGA.

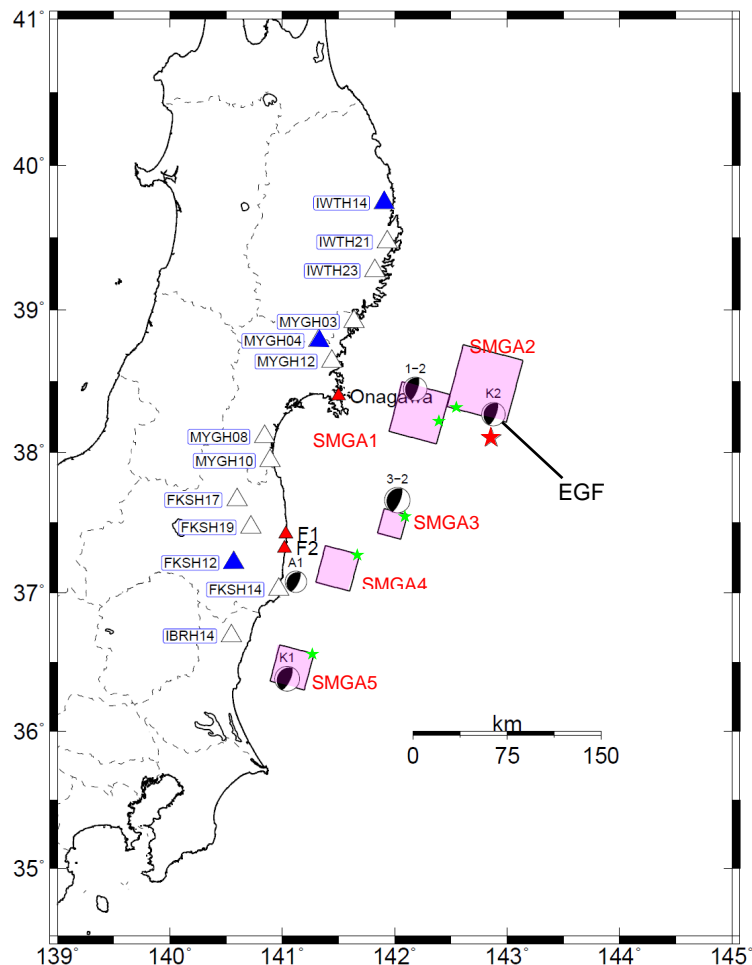


Figure 3. Map of SMGA (pink squares) distribution, the EGF earthquakes with their focal mechanisms (beach balls), the stations (triangle) used for analysis. Green stars are the rupture starting points and the red solid star means the epicentre of the main shock. The blue solid triangles mean the stations shown in Fig. 4 and 5.

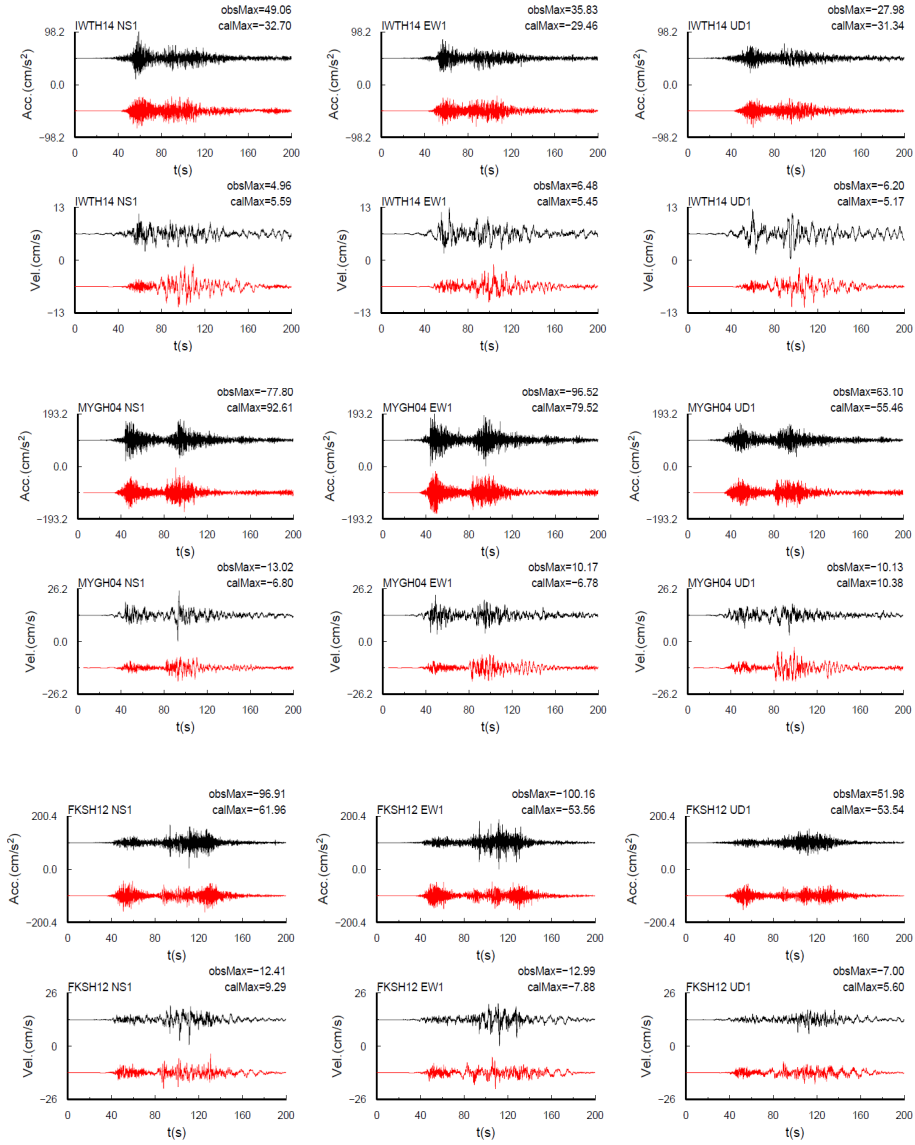


Figure 4. Examples of waveform comparison. Simulated acceleration and velocity waveforms (red) of three components (the NS, EW and UD components from the left to right) are compared with those observation ones (black) at IWTH14, MYGH04, and FKSH12 stations, respectively.

Forward simulations are conducted to develop the source model using the trial and error method. During the development, adjustment of position and source parameters of each SMGA is allowed, whereas the size of each SMGA and the rupture starting time are fixed. To construct an objective reproducibility criterion, we calculate the ratios of the averaged simulated response spectra to the observation spectra at three period bands, i.e., 0.1-0.5 sec, 0.5-2 sec, and 2-10 sec, respectively. While aiming at an overall simulation for all stations considered in this study (See Fig.3), special attention is paid to the reproducibility for the 0.1-0.5 sec band and particularly the strong motions observed around the NPP sites.

Table 1 lists the source parameters for each SMG as our final source model. In contrast to the slip model of Section 2, which is featured with the concentration of large slip in the shallow region east to the hypocenter, the strong-motion-generating source model consists of five source areas (SMGA) located in the deep region west to the hypocenter. The comparison of the simulation results (i.e., acceleration/velocity waveforms in Fig.4 and the response spectra in Fig. 5) with the observation data at representative stations indicates an excellent simulation by using our final source model. A quantitative comparison is shown in Fig.6, where the ratios of response spectra are plotted for the three period bands, respectively.

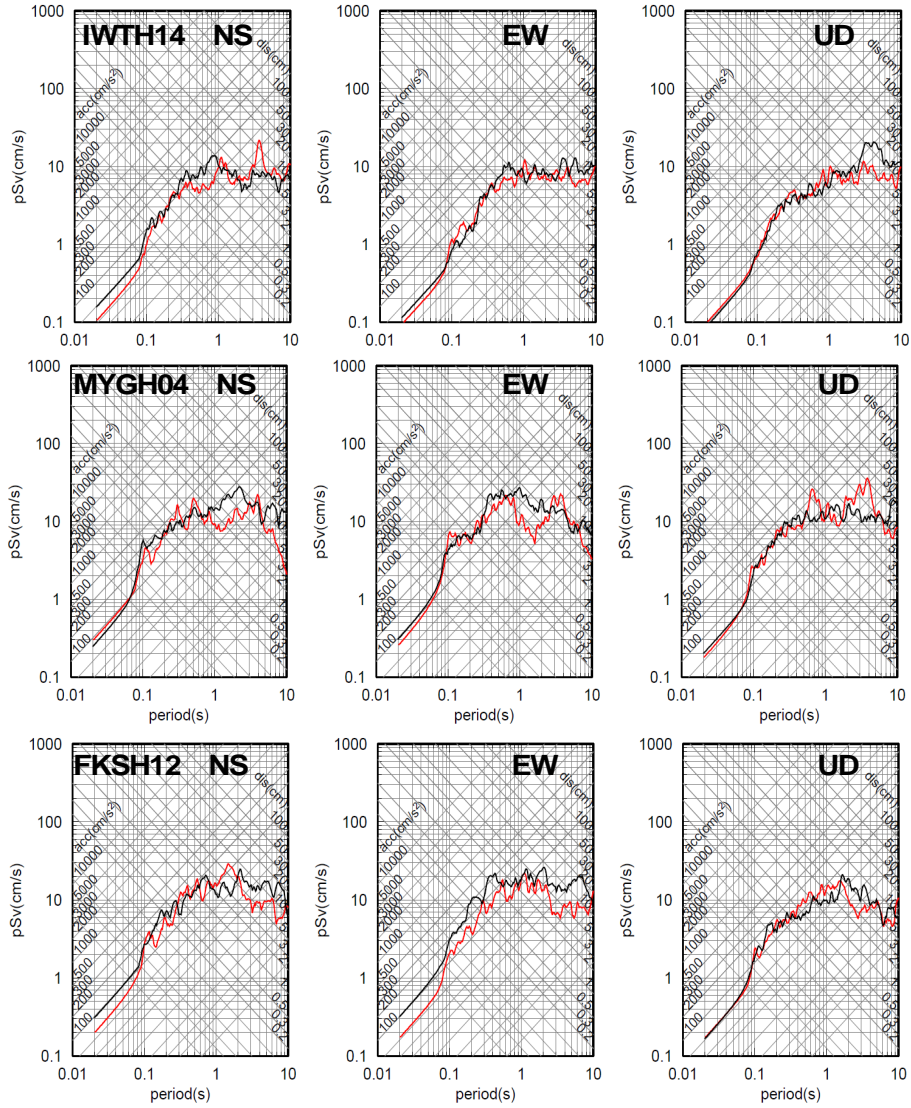


Figure 5. Examples of response spectrum comparison. The velocity response spectra (red) calculated from the simulation waveforms of three components (the NS, EW and UD components from the left to right) are compared with those observation ones (black) at IWTH14, MYGH04, and FKSH12 stations, respectively.

Table 1. Source parameters of each SMGA

	Length \times Width (km by km)	Depth to top (km)	Seismic Moment ($\times 10^{20}$ Nm)	Stress drop (MPa)	Dip (degree)	Time delay (sec)
SMGA1	40 by 40	25.4	4.93	28.4	17	0
SMGA2	50 by 50	15.1	11.0	21.6	17	35
SMGA3	20 by 20	25.1	0.88	27.0	19	57
SMGA4	30 by 30	28.7	1.19	10.8	22	87
SMGA5	30 by 30	28.3	2.58	23.1	20	102

Table 2. Source parameters of small events used for EGF

Event No.	Origin time	Latitude/Longitude (degree/degree)	Depth (km)	Seismic moment ($\times 10^{18}$ Nm)	Mw	Strike (deg)	Dip (deg)
1 (SMGA1)	2005/12/17 03:32	38.4487/142.1813	39.9	1.12	6.0	196;20	19;72
2 (SMGA2)	2011/03/10 03:16	38.2712/142.8788	28.9	1.10	6.0	201;22	19;71
3 (SMGA3)	2004/05/29 12:47	37.6615/142.0235	37.8	0.45	5.7	202;23	18;72
4 (SMGA4)	2005/10/29 22:46	37.0797/141.1205	52.0	0.21	5.5	217;26	22;69
5 (SMGA5)	2005/10/19 20:44	36.3817/141.0432	44.0	3.18	6.3	209;25	22;68

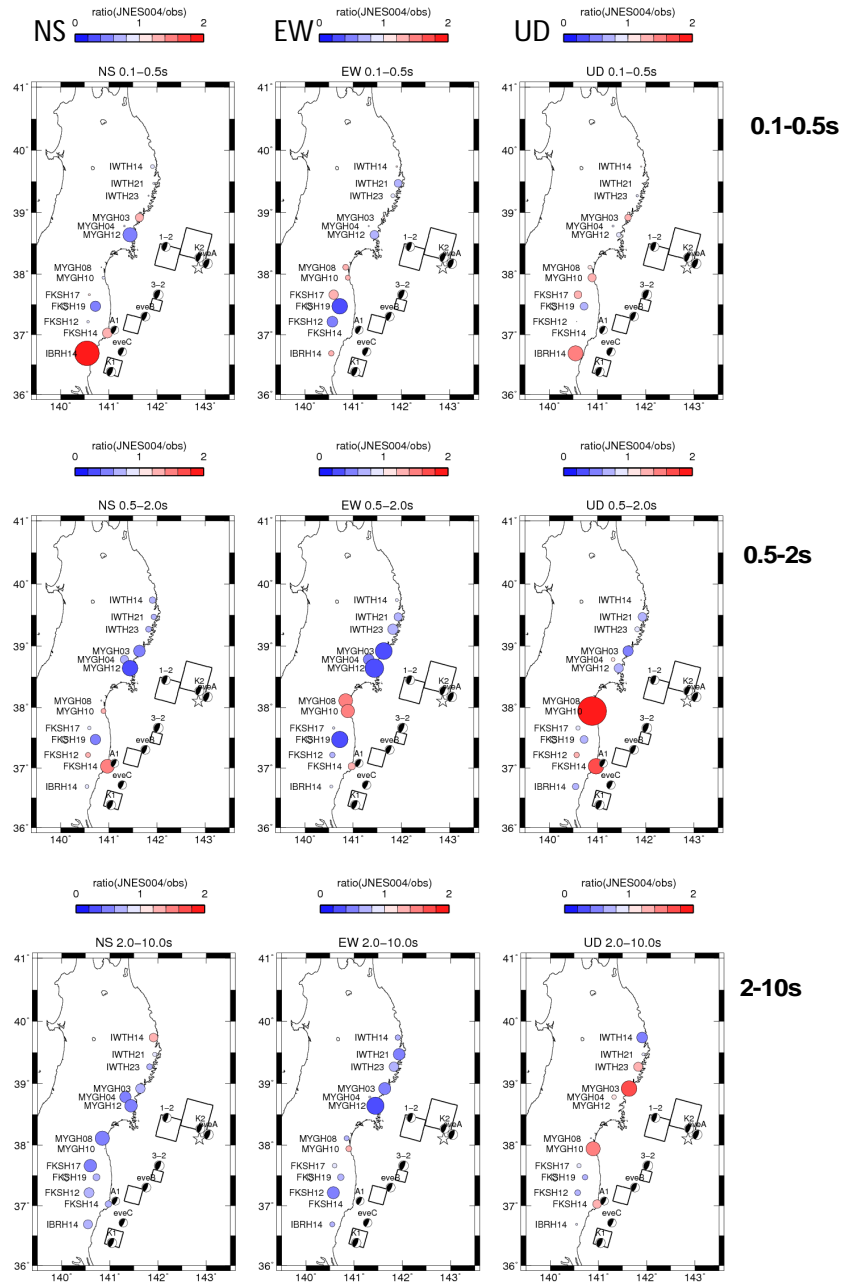


Figure 6. Period-band specific comparison of response spectrum ratios. Upper, middle, and lower are for the ratios of response spectra averaged for the period band of 0.1-0.5sec, 0.5-2sec, and 2-10 sec, respectively. The left, central, and right columns are for the NS, EW and UD components, respectively.

4. COMPARISON TO THE DBGGM AT THE ONAGAWA NPP SITE

As mentioned above, besides the method based on empirical prediction equations, DBGGMs are required by NSC to be formulated by using the source rupture modelling method. In this section, we apply the source modelling method to the assumed Miyagi-oki earthquake, a scenario earthquake which had been investigated by the HERP. This scenario earthquake was also considered for formulation of DBGGM for the Onagawa NPP site. Evaluation of ground motions from this scenario earthquake can be a test of validation of the NSC methodology. Following the NSC regulation guides, we consider the source model composed of simultaneous ruptures on the three fault planes as showed in Fig. 7. With uncertainties in the source parameters taken into account, stress drops of the asperities are raised to 1.5 times of the values used in the HERP model.

Short-period ground motions are calculated by applying the Stochastic Green's function method (Boore, 1983) and a total of 25 cases of short-period waves are considered to account the phase variability. The relatively long period (mainly larger 0.5sec) waveforms are computed by using analytical Green's functions (Hisada, 1997). The two-type ground motions are added together in time domain using the hybrid method (Irikura and Kamae, 1999), where a highpass filter is applied to the aforementioned short-period waveforms and a matched lowpass filter to the long-period ones. Table 3 and 4 list the main outer and inner source parameters of the used model. For definition of those source parameter and detailed procedure, refer to Irikura and Miyake (2012).

Following the abovementioned procedure, we evaluate the ground motions for the Onagawa site and compare them with the observation data (Fig. 8). Note that the response spectra of ground motions observed during the Tohoku earthquake at the Onagawa site (blue curves in Fig. 8) are in the range of those of the evaluation results. It suggests that the NSC method is valid and the source model of the Miyagi-oki scenario earthquake is efficient to appropriately evaluate the ground motions for seismic design even against a megathrust earthquake such as the Tohoku earthquake.

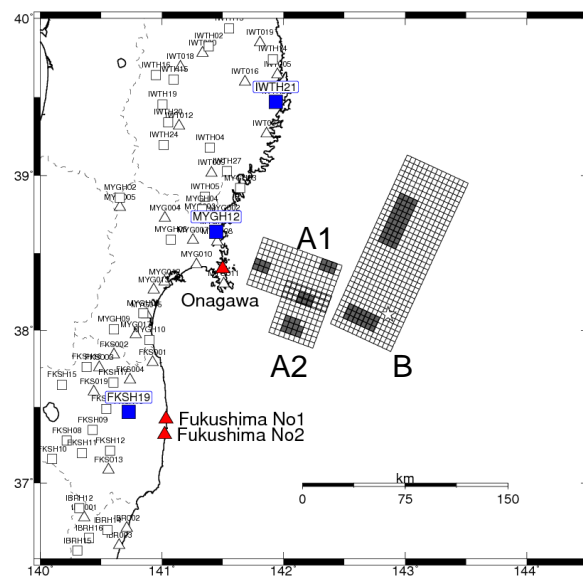


Figure 7. Fault geometry and asperity (dark black areas) distribution of the source model of the Miyagi-oki scenario earthquake used for verification.

Table 3. Outer source parameters of the Miyagi-oki scenario earthquake

Total Area (km ²)	Total Moment ($\times 10^{20}$ Nm)	Individual Area (km ²)			Stress drop (MPa)	Strike (deg)			Dip (deg)		
		A1	A2	B		A1	A2	B	A1	A2	B
9820	22.4	2304	1440	6517	5.6	200	200	205	20	20	12

Table 4. Inner source parameters of the Miyagi-oki scenario earthquake

	Seismic Moment ($\times 10^{20}$ Nm)	Average Slip (m)	Stress drop (MPa)	Rise time (sec)	Equivalent radius (km)
Asperity 1 on A1	96	5.45	43.5	1.13	5.53
Asperity 2 on A1	96	5.45	108.9	0.45	5.53
Asperity 3 on A1	96	5.45	95.4	0.51	5.53
Asperity on A2	184	7.55	82.7	0.82	7.65
Asperity 1 on B	549	13.03	53.1	2.21	13.22
Asperity 2 on B	274	9.21	53.1	1.6	9.34
Asperity Total	1295	9.76	63.9	-	20.30
Background	8525	4.13	5.15	7.24	-

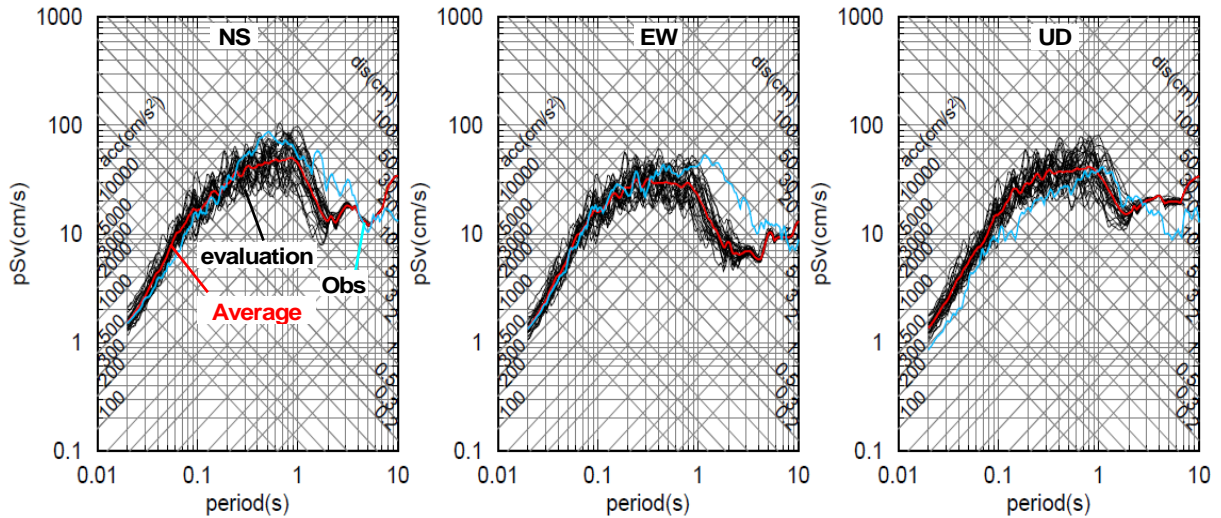


Figure 8 Response spectrum comparison of evaluated ground motions (black) with the seismic ground motions (blue) observed during the Tohoku earthquake. The red curves mean the average response spectra of the evaluated ground motions.

5. DISCUSSION AND CONCLUSIONS

Source models of the Tohoku earthquake are estimated from the long-period strong motions and the short-period motions, respectively. Inversion results of long-period waveforms give rise to the source model featured with large slip concentrated in the up-dip (shallow) region east to the hypocenter along the Japan trench. In contrast, the source model from strong (short-period) motion simulation is composed of five SMGA located in the down-dip (deep) region. This feature is also observed by other studies on the Tohoku earthquake (e.g., Lay et al., 2011). A tectonic model favouring this feature is to categorize the source area into two domains, i.e., the shallow region producing large slip but radiating very few seismic wave energy, and the deep region generating strong motions with large seismic wave energy even though the slip might be of moderate values (Lay et al., 2011).

Meanwhile, source characterization of the scenario earthquakes is based on the method proposed by Somerville (1999), where asperity configuration is inferred on the basis of slip distribution. Since slip distribution needs not be consistent with SMGA distribution, a new characterization method should be considered such that a consistent source model could be used both for ground motion and tsunami simulation. A possible direction to eliminate the gap between the long-period/tsunami source model and the SMGA model is to pay attention to the distribution of maximum slip rates instead of final slip in the case of ground motion simulation whereas the final slip distribution is important for tsunami or long-period ground motion simulation. A study on this issue is undergoing in the research projects of the Japan Nuclear Energy Safety Organization (JNES).

In conclusion, the Tohoku earthquake produced large slip in the shallow region along the Japan trench, consistent with the results of tsunami analysis. On the other hand, the short-period wave generation areas were confined in the deep region. The difference between the slip and SMGA distribution is of great importance for NPP seismic design since the seismic motions with potential damage to NPP safety are confined in the short-period region. It indicates that the goal of appropriate formulation of DBGM could be achieved by strict evaluation of near-site earthquakes like those in the Onagawa site. Ground motions evaluated for the Onagawa site using the Miyagi-oki scenario earthquake are of the same level as those observed during the Mw9.0 Tohoku earthquake. It follows that the level of strong motions was not out of expectation even though the earthquake magnitude and the wide range of source area were totally beyond previous estimations.

ACKNOWLEDGEMENT

This study is a part of JNES' emergency response to the Fukushima Daiichi accident. The K-NET and KiK-net seismograms of the 2011 Tohoku earthquake were distributed by the National Research Institute for Earthquake Science and Disaster Prevention.

REFERENCES

- Abdelwahed, M.F. and Zhao, D. (2007) Deep structure of the Japan subduction zone. *Phys. Earth Planet. Inter.* **162**, 32-52.
- Aoi, S., Obara, K., Hori, S., Kasahara, K., and Okada, Y. (2000). New strong-motion observation network: KiK-net. *Eos Trans. AGU*, **81**, Fall Meet. Suppl., Abstract S71A-05.
- Apel, E. V., Bu'rgmann, R., Steblov, G., Vasilenko, N., King, R., and Prytkov, A. (2006). Independent active microplate tectonics of northeast Asia from GPS velocities and block modeling, *Geophys. Res. Lett.*, **33**, L11303, doi:10.1029/2006GL026077
- Boore, D.M. (1983). Stochastic simulation of high-frequency ground motions based on seismological models of the radiated spectra, *Bull. Seism. Soc. Am.* **73:6**, 1865-1896.
- Hisada Y. (1997). Efficient methods for computing Green's functions and normal mode solutions for layered half-spaces. *J. Struct. Constr. Eng. AIJ* **501**, 49-56.
- International Atomic Energy Agency (2008). Mission Report: 2nd follow-up IAEA mission in relation to the findings and lessons learned from the 16 July 2007 earthquake at Kashiwazaki-Kariwa NPP, http://iaea.org/newscenter/news/pdf/kashiwazaki011208_vol1.pdf.
- Irikura, K. (1994). Earthquake source modeling for strong motion prediction. *Zishin -2* **46**, 495-512 (in Japanese with English abstract).
- Irikura, K. and Kamae K. (1998). Strong ground motions during the 1948 Fukui earthquake: Estimation of broadband ground motion using a hybrid simulation technique. *Zishin-2* **52**, 129-150.
- Irikura, K. and Miyake, H. (2001). Prediction of strong ground motions for scenario earthquakes, *Journal of Geophraphy* **110**, 849-875 (in Japanese with English abstract).
- Irikura, K. and Miyake, H. (2010). Recipe for predicting strong ground motion from crustal earthquake scenarios. *Pure and Applied Geophysics*, doi:10.1007/s00024-010-0150-9.
- Kawabe, H., Kamae, K. and Uebayashi, H. (2011). Source modeling of the 2011 Tohoku-chiho Taiheiyo-Oki earthquake, *Japan Geoscience Union Meeting 2011*, MIS036-P35.
- Kennett, L. N. and Kerry, N. J. (1979). Seismic waves in a stratified half space, *Geophys. J. R. Astron. Soc.* **57**, 557-583.
- Kinoshita, S. (1998). Kyoshin Net (K-NET), *Seismol. Res. Lett.* **69**, 309-332.
- Kurahashi, S. and Irikura, K. (2011). Source model for generating strong ground motions during the 2011 off the Pacific coast of Tohoku earthquake. *Earth Planets Space* **63**, 571-576
- Lay, T., Ammon, C.J., Kanamori, H., Kim, M., and Xue, L. (2011). Outer trench-slope faulting and the 2011 Mw 9.0 off the Pacific coast of Tohoku earthquake. *Earth Planets Space* **63**, 713-718.
- Nishimura, T., Hirasawa, T., Miyazaki, S., Sagiya, T., Miura, S. and Tanaka, K. (2004). Temporal change of interpolate coupling in northeastern Japan during 1995-2002 estimated from continuous GPS observations. *Geophys. J. Int.*, **157**, doi:10.1111/j.1365-246X.2004.02159.x.
- Shinohara, M., Hino, R., Yoshizawa, T., Nishino, M., Sato, T., and Suyehiro, K. (2005). Hypocenter distribution of plate boundary zone off Fukushima, Japan, derived from ocean bottom seismometer data. *Earth Planets Space* **57**, 93-105.
- Somerville, P., Irikura, K., Graves, R., Sawada, S., Wald, D., Abrahamson, N., Iwasaki, Y., Kagawa, T., Smith, N. and Kowada, A. (1999). Characterizing crustal earthquake slip models for the prediction of strong ground motion. *Seismological Research Letters* **70:1**, 59-80.
- Sugino, H., Iwabuchi, Y., Nemoto, M., Korenaga, M., and Ebisawa, K. (2012). Investigation of mechanisms causing ground motions and tsunami due to the 2011 Tohoku earthquake at Nuclear Power Plant sites, *Proceedings of the 15th World Conference on Earthquake Engineering*, Lisbon, Portugal (this conference).
- Wu, C., Koketsu, K., and Miyake, H. (2008). Source processes of the 1978 and 2005 Miyagi-oki, Japan, earthquakes: Repeated rupture of asperities over successive large earthquakes. *J. Geophys. Res.*, **113**, B08316, doi:10.1029/2007JB005189.
- Wu, C., Minoru, T. and Ide, S. (2001). Source process of the Chi-Chi earthquake: A joint inversion of strong motion data and Global positioning system data with a multifault model. *Bull. Seism. Soc. Am.* **91:5**, 1128-1143.
- Yamanaka, Y. and Kikuchi, M. (2004). Asperity map along the subduction zone in northeastern Japan inferred from regional seismic data. *J. Geophys. Res.*, **109**, B07307, doi:10.1029/2003JB002683.
- Yokoi, T. and Irikura, K. (1991). Empirical Green's function technique based on the scaling law of source spectra. *Zishin-2* **44**, 109-122.